

## Compact and Dissociated Dislocations in Aluminum: Implications for Deformation

S. G. Srinivasan,\* X. Z. Liao, M. I. Baskes, R. J. McCabe, Y. H. Zhao, and Y. T. Zhu

Materials Sciences Division, Los Alamos National Laboratory, Los Alamos, NM 87545, USA

(Received 3 May 2004; published 30 March 2005)

Atomistic simulations, confirmed by electron microscopy, show that dislocations in aluminum can have compact or dissociated cores. The calculated minimum stress ( $\sigma_p$ ) required to move an edge dislocation is approximately 20 times smaller for dissociated than for equivalent compact dislocations. This contradicts the well accepted generalized stacking fault energy paradigm that predicts similar  $\sigma_p$  values for both configurations. Additionally, Frank's rule and the Schmid law are also violated because dislocation core energies become important. These results may help settle a 50-year-old puzzle regarding the magnitude of  $\sigma_p$  in face-centered-cubic metals, and provide new insights into the deformation of ultra-fine-grained metals.

DOI: 10.1103/PhysRevLett.94.125502

PACS numbers: 61.72.Lk, 62.20.Fe, 62.25.+g

Materials' yield strength, or the maximum load a material can support without permanent (plastic) deformation, is an important property [1]. Plastic deformation is both a fundamental technological asset for producing shape change during materials forming and a precursor to material failure. It relates to the ease of moving crystal defects called dislocations [1]. Dislocation motion in metals occurs at stresses many orders of magnitude below their theoretical bond strength. Thus, practical means of enhancing material strength involve creating internal obstacles to dislocation motion such as precipitates, other dislocations, and/or grain boundaries [1].

Dislocations provide a fundamental framework to understand the strength of metals. The self-energy of a dislocation is proportional to the square of its Burgers vector  $\mathbf{b}$ . According to Frank's rule, it is energetically favorable for this dislocation to split into two partial dislocations with Burgers vectors  $\mathbf{b}_1$  and  $\mathbf{b}_2$  if  $b^2 > (b_1^2 + b_2^2)$ . In coining this simple rule, Frank implicitly assumed the energy of dislocation core, the region where atoms are displaced most from their perfect crystal positions, to be negligible. In face-centered-cubic (fcc) metals dislocations usually split into two Shockley partials with a planar core confined to a  $\{111\}$  slip plane, and enclose a stacking fault (SF) region with hexagonal-close-packed (hcp) structure. The energy of this SF region largely determines the splitting width. For example, in Al, a high stacking fault energy fcc metal, the splitting width is observed to be around 0.55 nm for  $60^\circ$  dislocations [2] (yielding 0.58 nm for a lattice edge dislocation [1]).

In this Letter we report atomistic simulations and high-resolution electron microscopy (HREM) experiments on the core structure of dislocations in Al and examine its effects on dislocation glide. We find that in Al, the dislocation core may either be *compact* or *dissociated* (see Table I). Atomistic simulations also revealed that the Peierls stress ( $\sigma_p$ ), the intrinsic lattice resistance to dislocation motion, is about 20 times smaller for the glide of dissociated edge dislocations than for equivalent compact dislocations. These results reveal a new approach to inhibit

dislocation motion in some fcc metals by tailoring compact core structures. They may also shed light on a 50-year-old puzzle wherein a factor of 100 discrepancy exists between the  $\sigma_p$  of fcc metals estimated from the Bordoni peak (BP) internal friction measurements and those obtained from mechanical testing [3–5]. Further, they unequivocally show that in high SF energy metals like aluminum, the core effects become significant and thus we cannot use a SF energy criterion to determine the splitting width. In such situations we need to explicitly determine core widths of dislocations from full atomistic calculations. Importantly, we have presented an intriguing concept of multiple dislocation cores that may be applicable for metals in general.

*Atomistic simulations.*—We first compare and contrast atomistic simulations of edge dislocations in Al using two state-of-the-art embedded atom method (EAM) potentials [6,7]. These potentials, Ercolessi and Adams (EA) and Baskes *et al.* (BAM), are excellent in their representation of properties of Al relevant to dislocation behavior, such as energy *versus* volume, equilibrium lattice constant, elastic moduli, vacancy formation energy, stacking fault energy, and the generalized stacking fault (GSF) curve. While the BAM potential was obtained by fitting to experimental properties of Al, the EA potential was developed by fitting parameters to both experimental properties and to a large database of forces obtained from quantum mechanical calculations.

Molecular statics (MS) was used to study dislocation core structures and energy. A 8.6 nm diameter cylinder with 1.5 nm period along the dislocation line was used.

TABLE I. Comparing the DFT, experiment, and EAM stacking fault energy (SFE) in  $\text{J/m}^2$  and edge dislocation widths in nm. Dislocation width in DFT was estimated from SFE.

	DFT <sup>15</sup>	Experiment	BAM	EA
SFE	0.16	0.14–0.16 <sup>1</sup>	0.10	0.12
Width	0.32	0.62, 0.5/4.0 <sup>12</sup>	0.5/1.5	1.6

Dislocations were introduced into the model using displacements calculated from anisotropic elasticity theory. Atoms within two cutoff distances of the cylinder surfaces were fixed while the energy of inner atoms was minimized using a conjugate-gradient method [7]. Minimized systems had average forces of  $<10^{-5} \frac{\text{eV}}{\text{nm}}$ . Nearly identical dislocation core structures resulted from MS and molecular dynamics (MD) simulations.

To investigate dislocation motion, MD simulations were carried out at 10 K using a Nosé-Hoover thermostat [8]. The simulation cell had 6900 atoms and was periodic along the  $X$  and  $Y$  directions. The dislocation line and the slip plane normal were parallel to the  $Y$  and  $Z$  axes, respectively. The box edges along the  $X$ ,  $Y$ , and  $Z$  axes were 17.4, 1.6, and 5.0 nm, respectively. This geometry represents an infinite array (in the  $X$  direction) of straight dislocations. Shear stresses were imposed by applying forces in the  $X$  direction to two layers at the top and bottom  $Z$  surfaces. The minimum stress to move the dislocation is the  $\sigma_P$ . A cell with  $\approx 50\,000$  atoms also yielded similar results.

Figure 1 shows the GSF energy curves of BAM and EA Al along  $\langle 211 \rangle$  are similar. Using the GSF for the EA potential and a *modified* Peierls-Nabarro (PN) model, Lu *et al.* [9] calculated  $\sigma_P$  for an edge dislocation to be 24 MPa. However, our MD calculations show that the  $\sigma_P$  needed to move a *lattice* edge dislocation is approximately

1 MPa for EA Al and 225 MPa for BAM Al. These differences in  $\sigma_P$  conflict with the assumption that the GSF curve determines dislocation mobility.

The large difference in  $\sigma_P$  is caused by different ground state configurations for edge dislocations in EA and BAM Al (Fig. 2). For the EA Al, a lattice edge dislocation spontaneously splits into two Shockley partials separated by about 1.6 nm. Although we initially created a lattice dislocation, we end up moving a dissociated dislocation in EA Al at low  $\sigma_P$ . In contrast, for BAM Al, a lattice dislocation does not spontaneously dissociate into Shockley partials but retains a compact core  $\sim 0.5$  nm wide, and we must apply a large stress to move this compact dislocation.

In BAM Al, two Shockley partials, initially separated by  $>0.5$  nm, move to a final separation of 1.5 nm, yielding a dissociated core. To determine the dislocation core energy ( $\xi_c$ ), we used MS.  $\xi_c$  is defined as the intercept of the straight line plot of system energy versus  $\log(R)$ , where  $R$  is the distance from the dislocation line. The  $\xi_c$  of the compact BAM dislocation is 521 pJ/m, which is 27 pJ/m below the dissociated dislocation, indicating that the dissociated dislocation is a *metastable* configuration thus violating Frank's rule [1]. This energy difference is about 5% of the compact dislocation core energy.

The dissociated dislocation in BAM Al moves at  $\sigma_P \approx 13$  MPa, 20 times less than the  $\sigma_P$  for the compact BAM dislocation. Thus the BAM dissociated dislocation moves at a stress comparable to the EA Al (and experiments) while the compact dislocation moves at a much larger applied stress. The lower  $\sigma_P$  of dissociated dislocations compared to their compact counterparts has been suggested before, but has never been demonstrated until now [1,4]. The *classical* PN model, based on continuum dislocation theory, also predicts  $\sigma_P$  to increase with decreasing dislocation core width as:  $\sigma_P = \mu \exp(-4\pi\zeta/b)$ , where  $\zeta$  is the core radius,  $b$  the magnitude of the Burgers vector, and  $\mu$  the shear modulus. However, the

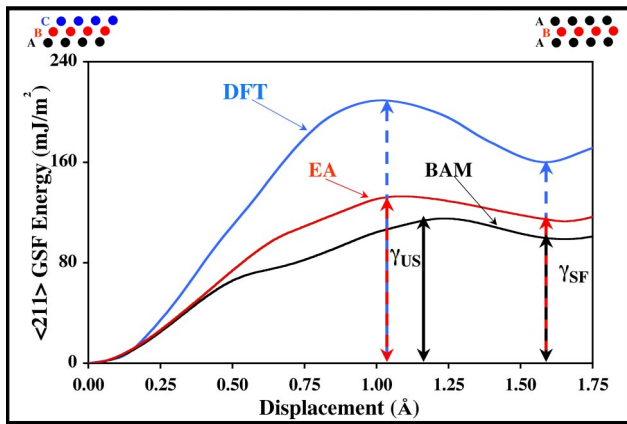


FIG. 1 (color online). The relaxed GSF energy curves along  $\langle 211 \rangle$  for DFT, BAM, and EA Al potentials. The GSF energy paradigm elegantly unifies the dislocation splitting and core phenomena, and relates dislocation motion to  $\sigma_P$  [16,17]. The GSF curves shown here were obtained by cutting the fcc crystal parallel to a  $\{111\}$  plane and displacing the top half rigidly over the bottom half along  $\langle 211 \rangle$ , allowing for relaxation along  $\langle 111 \rangle$ . While the peak positions for the unstable SF energy ( $\gamma_{US}$ ) for the two curves do not coincide, by symmetry the stable SF energy ( $\gamma_{SF}$ ) occurs at the same displacement for the three potentials. The DFT derived  $\langle 211 \rangle$  GSF curve (taken from [9]) has higher  $\gamma_{SF}$  and  $\gamma_{US}$  than BAM and EA. However, the maximum slope of these curves, a measure of the Peierls stress, is not very different. The left and right inset figures show the  $\{111\}$  planar stacking for the fcc (ABC) and hcp (ABA).

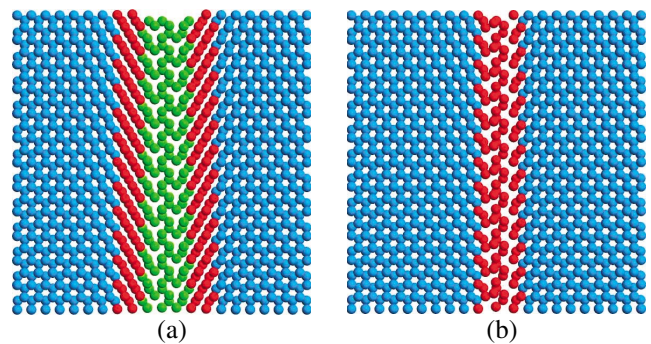


FIG. 2 (color online). Dissociated (a) and compact (b) edge dislocations with  $\mathbf{b} = \mathbf{a}/2[0\bar{1}1]$ , viewed on (111) plane. Their SF widths are, respectively, 1.6 nm and 0.5 nm. We used common neighbor analysis [18] to identify bulk and dislocation core atoms (blue = fcc, green = hcp, and red = unknown atom).

$\sigma_P$  values for compact and dissociated dislocations predicted by this model are many orders of magnitude smaller than the values obtained from MD.

Figure 3 shows dislocation position versus time for EA Al and both compact and dissociated dislocations in BAM Al. Also shown as a function of time are the number of hcp atoms in the dislocation core, a direct measure of the stacking fault width. Both edge and screw dislocations in EA Al move steadily at 1 MPa applied resolved shear stress with little change in the core width. The  $\sigma_P$  for the screw dislocation in EA Al is significantly lower than 82 MPa calculated by Bulatov *et al.* [10]. We believe this discrepancy is caused by the smaller core width of 0.49 nm obtained by them due to their boundary conditions (our MS calculations show the EA screw dislocation splits to 1.6 nm). In contrast, the edge dislocation motion in BAM Al shows various mobilities. Interestingly, there is a direct correlation between dislocation mobility and the number of hcp atoms. At small stresses, the dislocation motion is hindered, and in extreme cases totally arrested, when the number of hcp atoms becomes zero yielding a compact core. The reverse of this process is also seen. Thus, a transition between the two core states can occur during dislocation motion even at low temperature.

For BAM Al, using MS in a cylindrical geometry, we also discovered that a shear stress parallel to the dislocation line acts on the screw component of the partial dislocations and alters the core configuration. By applying such a shear stress of at least 600 MPa, the BAM compact core splits into the dissociated core. However, reversing the direction of shear stress did not *fully* collapse the dissociated core into a compact core. The transition between the compact and dissociated core states by temperature and/or stress illustrates non-Schmid behavior. The energetics of the transition from the compact to dissociated states have been calculated for the BAM Al using a chain-of-states method [11]. The stresses for the transition are consistent with that found by MS.

**HREM experiments.**—Aluminum has a high SF energy (Table I) and past experiments indicate a compact dislocation core with no evidence of SFs [1,2]. So the crucial question is: do our MD predictions of compact and dissociated dislocations relate to real Al? To answer this question we characterized cryogenically deformed *polycrystalline* Al samples using HREM. To prepare the sample, we shoot steel balls (“shot-peening”) at a 99.99% pure Al sheet at liquid nitrogen temperature. This produced a microstructure with equiaxed and elongated grains (sizes between 0.2–1.0  $\mu\text{m}$ ). HREM results unequivocally show large densities of compact and dissociated dislocations *inside* small and large Al grains (Fig. 4), corroborating our simulations. Similar results were obtained in ball-milled, *nanocrystalline* Al (99.99% pure) [12].

HREM results show that there is a large spread in the SF widths [12]. The average width of dissociated dislocations in our experiments was 4 nm and in our simulations it was 1.5 nm. HREM is known to overestimate the width of the SF and so we also examined our shot-peened Al samples by tilting them under weak-beam imaging, a method that underestimates the SF width. However, weak-beam experiments were hard to perform because of small grain size in the sample. Preliminary results indicate that the SF width lies in the 3–4 nm range.

Earlier, HREM studies of Mills and Stadelmann [2] determined the SF widths of 60° dislocations in undeformed Al single crystal to be 0.55 nm. This width is comparable to that of our compact dislocation but much smaller than that of the dissociated EA or BAM dislocations. The higher than expected width of dissociated dislocations in our HREM studies may be reconciled as follows. HREM experiments use Al foil. The split dislocation runs from the back face of the foil to its front face and may be inclined giving the appearance of a wider splitting. Further, we wish to emphasize that, unlike the single crystal studies in Ref. [2], we examined deformed ultra-fine-grained (UFG) Al samples. We acknowledge that

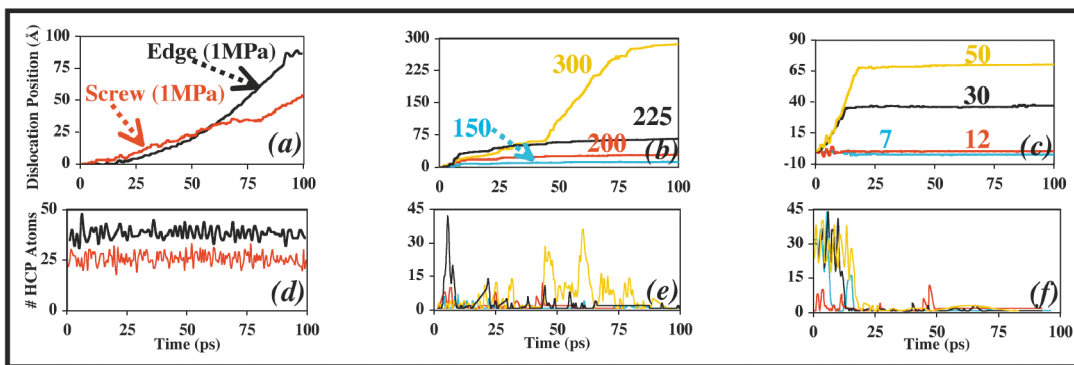


FIG. 3 (color). (a)–(c) show dislocation position vs time at indicated resolved shear stress (MPa): (a) shows EA edge and screw dislocations, (b) BAM compact edge dislocation, (c) BAM dissociated edge dislocation. (d)–(f) show the number of hcp atoms, in dislocation core, vs time for curves shown in (a)–(c). The color coding is same as (a)–(c). There is a direct correlation between the number of *hcp* atoms and dislocation motion. When *hcp* atoms disappear, i.e., *core collapses*, the dislocation motion stops.

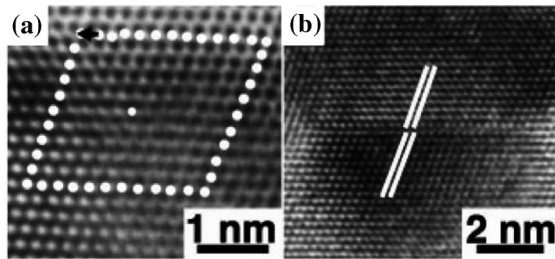


FIG. 4. HREM of cryogenically deformed 99.99% pure UFG Al viewed along  $\langle 110 \rangle$ . (a) A compact  $60^\circ$  lattice dislocation. A white dot marks the dislocation core at the image center. A Burgers circuit and closure failure is also marked. An extra half plane is evident. (b) A dissociated dislocation with SF between the two Shockleys. Parallel white straight lines indicate the lattice shift caused by the SF.

the presence of small grains and/or internal stresses affects the relative proportions of compact and dissociated dislocations, thus possibly explaining why only compact dislocations were seen in single crystal studies. It is possible that the compact dislocations observed by Mills and Stadelmann [2] were much less mobile than the dissociated ones and only they remained in the HREM foil.

The predictability and limitations of EAM potentials are well known [7]. *Ab initio* methods are definitely more accurate than semiempirical EAM potentials for modeling dislocations. However, computational limitations currently prohibit large-scale *ab initio* dislocation calculations. Thus we used two EAM models that predict many properties of Al well, especially its large stacking fault energy, lattice, and elastic constants relevant to our dislocation modeling. Although the exact values of the stacking fault energies are irrelevant to the results presented here, the BAM and EA models nevertheless predict the stacking fault energies to lie within the wide scatter of experimental values (Table I).

*The Peierls stress controversy.*—The  $\sigma_P$  from BP measurements in Al ( $=200$  MPa) is about 2 orders of magnitude larger than the  $\sigma_P$  from mechanical tests. Such discrepancy exists for other fcc metals and has caused a long-lasting controversy on the magnitude of  $\sigma_P$  for fcc metals [3–5,13,14]. For body-centered-cubic (bcc) metals and ionic crystals there is, however, no such discrepancy [3–5]. Underlying this controversy is the unfortunate fact that a model, whose details are important, must be used to relate the experiment and  $\sigma_P$ . Furthermore, more recently, Kosugi and Kino [5] discovered a low temperature (11 K) BP in ultra high-purity Al. The  $\sigma_P$  value computed from this peak is comparable to that estimated from mechanical testing. Addressing this controversy, Lauzier *et al.* [14] surmised that vacancies generated from cold-work may, surprisingly, enhance dislocation mobility. Using a modified PN model with an *ab initio* determined  $\gamma$  surface, Lu and Kaxiras [15] show an order of magnitude lowering of  $\sigma_P$  attributed to increased dislocation splitting due to vacancies. However, while the experiments [14] had only a few

atomic ppm vacancies, these simulations [15] contained four atomic % vacancies—much larger than the vacancy concentration generated in cold work. Another serious deficiency of this work is the absence of dislocation pinning interstitials also produced by cold work. Our results, without invoking such effects, show the compact core dislocation in BAM Al has a  $\sigma_P$  consistent with the initial BP measurements and the dissociated core with the 11 K BP. Thus, if the relationship between  $\sigma_P$  and BP is correct, core effects become important in many fcc metals. Earlier, Takeuchi [4] postulated such a scenario to reconcile the  $\sigma_P$  discrepancy.

Since Al is a high SF metal, we expect similar core effects to occur in other high SF energy materials. However, we admit it is hard to imagine, but harder to rule out, that these core effects would be strong enough in low SF energy metals to fully collapse the dislocation core.

We thank J. W. Cahn, P. S. Follansbee, R. G. Hoagland, T. E. Mitchell, and J. G. Swadener for their thoughtful comments. This work was sponsored by the U.S. Department of Energy, Office of Science.

\*Corresponding author.

Email: sgsrini@lanl.gov

- [1] J. P. Hirth and J. Lothe, *Theory of Dislocations* (Wiley, New York, 1982), 2nd edition.
- [2] M. J. Mills and P. Stadelman, *Philos. Mag. A* **60**, 355 (1989).
- [3] G. Fantozzi, C. Esnouf, W. Benoit, and I. G. Ritchie, *Prog. Mater. Sci.* **27**, 311 (1982).
- [4] S. Takeuchi, *J. Phys. Soc. Jpn.* **64**, 1858 (1995).
- [5] T. Kosugi and T. Kino, *J. Phys. Soc. Jpn.* **58**, 4269 (1989).
- [6] F. Ercolessi and J. B. Adams, *Europhys. Lett.* **26**, 583 (1995).
- [7] M. I. Baskes, J. E. Angelo, and N. R. Moody, in *Hydrogen Effects in Materials*, edited by A. W. Thompson and N. R. Moody (The Minerals, Metals and Materials Society, Warrendale, PA, 1996), pp. 77–85.
- [8] W. G. Hoover, *Phys. Rev. A* **31**, 1695 (1985).
- [9] G. Lu, N. Kioussis, V. V. Bulatov, and E. Kaxiras, *Phys. Rev. B* **62**, 3099 (2000).
- [10] V. V. Bulatov, O. Richmond, and M. V. Glazov, *Acta Mater.* **47**, 3507 (1999).
- [11] G. Mills, H. Jónsson, and G. K. Schenter, *Surf. Sci.* **324**, 305 (1995).
- [12] X. Z. Liao, S. G. Srinivasan, Y. H. Zhao, M. I. Baskes, Y. T. Zhu, F. Zhou, E. T. Lavernia, and X. F. Xu, *Appl. Phys. Lett.* **84**, 3564 (2004).
- [13] A. Seeger, *Philos. Mag.* **1**, 651 (1956).
- [14] J. Lauzier, J. Hillairet, G. Gremaud, and W. Benoit, *J. Phys. Condens. Matter* **2**, 9247 (1990).
- [15] G. Lu and E. Kaxiras, *Phys. Rev. Lett.* **89**, 105501 (2002).
- [16] V. Vitek, *Prog. Mater. Sci.* **36**, 1 (1992).
- [17] J. R. Rice, *J. Mech. Phys. Solids* **40**, 239 (1992).
- [18] H. Jónsson and H. C. Andersen, *Phys. Rev. Lett.* **60**, 2295 (1988).